Land surface temperature retrieval from HJ-1B satellite thermal infrared data and error analysis using partial differential equation

Jianbo Xu, Zhifeng Xiao*, Linyi Zhong, Kai Zhao and Ziyu Huang

College of Informatics, South China Agricultural University, Guangzhou, China

_____

ABSTRACT

In this study, we retrieved the land surface temperature (LST) of Guangzhou on Jan 14, 2013 from HJ-1B satellite data. The retrieval was based on the characteristics of HJ-1B thermal infrared band and revised QK&B algorithm was adopted. The established partial differential equation showed that emissivity error of 0.01 resulted in LST error of around 0.6 K. The LST error was inversely proportional to the atmospheric transmittance and proportional to the atmospheric transmittance error; The transmittance error of 0.1 resulted in LST error of around 1 K. Meanwhile, the atmospheric water vapor error and the LST error exhibited a linear relationship; The atmospheric water vapor error of 0.1 g/cm^2 resulted in LST error of around 0.2 K. The LST retrieval error was proportional to both the near-surface air temperature error and the average atmospheric error; The near-surface air temperature error of 1 K led to the LST retrieval error of around 1 K. Overall, at a constant ratio relation between emissivity and atmospheric transmittance, the LST retrieval error are related to the average atmospheric temperature error as well as the near-surface air temperature error. The retrieved land surface temperature of Guangzhou was in strong spatial accordance with the MOD11_L2 LST product. The temperature difference curve exhibited a normal distribution, concentrating in the range of -0.9K to 0.9K. Six observation areas in Guangzhou were chosen to compare the LST obtained by the revised QK&B algorithm with the measured average land surface temperature. The difference between the LST obtained using the algorithm and the measured temperature was around 0.31 K, whereas the MOD11_L2 product had a difference of around 0.65 K with the measured surface temperature, both of them are less than 1 K. By deriving the partial differential equations of the revised QK&B algorithm, a more detailed and precise analysis was performed on the LST retrieval from HJ-1B/IRS data. This study offers a reference for similar LST retrieval algorithms based on thermal infrared band of environmental satellites, as well as a scientific basis for future accuracy improvement of LST retrieval.

Key words: Revised QK&B algorithm; partial differential equation; sensitivity analysis; algorithm validation; HJ-1B

_____

INTRODUCTION

HJ-1B satellite is one of the small satellite constellations that China launched in 2008 for the purpose of environment and disaster monitoring and forecasting. This satellite carries a visible light camera and an infrared camera. Its infrared sensor (HJ-1B/IRS) only detects one thermal infrared band, with a resolution of 300 m, a wavelength range of 10.5 – 12.5 um and a scanning width of 720 km. The revisit period of HJ-1B is 96 h. During its operation, the satellite obtains the spatial distribution of the Earth's land surface temperature, which plays an important role in resource and environment monitoring[1]. Different applications of surface temperature data generally require different precisions of the data. For example, in the study of climate change, large-scale water surface temperature data should not contain errors that are greater than 0.3 K, whereas medium- and small-scale land surface temperature data allow error in the range of 0.5 – 1.0 K. Therefore, great attention has been paid to the factors that influence the accuracy of land surface temperature (LST) retrieval.

Currently, the most basic way to retrieve LST from thermal infrared remote sensing images is to generate single-channel, multi-channel and multi-angle retrieving models by solving equations of thermal infrared radiative transfer [2-4]. Generally, single-channel algorithms include radiative transfer equation (RTE) algorithm, Qinzhihao's single-channel algorithm (known as QK&B algorithm), and Jimenez-Munoz & Sobrino's (JM&S) single-channel algorithm. The RTE algorithm requires complicated computation and a considerable number of parameters, thus it is more difficult to be applied comparing with the other two algorithms, especially when real-time atmospheric profile is lacking. The JM&S algorithm and QK&B algorithm only require surface temperature, atmospheric water vapor content, and emissivity to retrieve LST [5-8]. Duan *et al.* [9] applied these two algorithms to simulate LST using data from HJ-1B, and concluded that JM&S algorithm produced higher accuracy. However, they only performed simple statistical analysis and derivation without thorough and substantive investigation. Although many scholars have conducted LST retrieval from HJ-1B/IRS data [10-14], most of the error analysis was based on statistical analysis of the data [9, 15-17]. Evaluation of the sensitivity and precision of error analysis using partial differential equation has rarely been reported.

In this study, based on the mechanism of thermal infrared, a revised QK&B algorithm was used to retrieve LST from HJ-1B thermal infrared data. Partial differential equations were established to analyze the error in LST retrieval, and the influence of each parameter' variation on the retrieval error was studied. This study offers a reference for similar LST retrieval algorithms that are based on thermal infrared data from environmental satellites, as well as a scientific basis for further accuracy improvement of LST retrieval.

REVISED QK&B AlGORITHM AND ITS PARAMETERS

Based on the equation of land surface thermal radiative transfer, Qin [18] derived an LST retrieval algorithm that is based on remote sensing with single infrared channel. This algorithm is known as the QK&B algorithm, and its formula is

$$\left\{ T_s = \frac{1}{C}[a(1-C-D)+T_{sensor}(b(1-C-D)+C+D)-DT_a] \right. \tag{1}$$

where T_s is the surface temperature (K), T_{sensor} is the temperature corresponding to satellite radiance, ε is the emissivity, *a* and *b* are constants with values of -68.035 and 0.46372, respectively, and $C = \varepsilon\tau$, $D = (1-\tau)[1+(1-\varepsilon)\tau]$, where τ is the atmospheric transmittance. The absolute radiometric calibration coefficients published by China Centre for Resources Satellite Data and Application in 2011 were used for calibration, in order to calculate the satellite radiance of the infrared band of HJ-1B/IRS. The following formulae were used.

$$\left\{ \begin{array}{l} L_{sensor} = (DN - 12.625)/56.277 \\ T_{sensor} = 1249.91/\ln(1+589.33/L_{sensor}) \end{array} \right. \tag{2}$$

where *DN* is the gray level of the IRS images, L_{sensor} is the satellite radiance, and T_a is the average atmospheric operative temperature. For HJ-1B satellite, an approximation formula of T_a, proposed by Qin [18], is $T_a = 24.70005 + 0.88894 T_0$, where T_0 is the near-surface temperature.

Xu *et al.* [19] adopted the temperature-vegetation index (TVX) approach to retrieve near-surface temperature in northwest China using HJ-1B remote sensing data. The result had mean absolute error (MAE) of 2.16 K and mean square root error of 2.72 K, indicating high accuracy. Therefore, the TVX approach was adopted in this study to retrieve near-surface temperature. The calculation of is T_0 illustrated below.

$$\begin{cases} T_0 = T_{min} + (T_{max} - T_{min})sin\left[\dfrac{\pi(t_h + dl/2 - 12)}{(dl + 2p)}\right] \\[2mm] dl = 12\left(1 + \dfrac{2}{\pi}sinLATsin\delta \, sin\dfrac{sinLATsin\delta}{cosLATcos\delta}\right) \\[2mm] sin\delta = -sin\left(23.45\pi/180\right)cos\left(2\pi\left(DOY + 10\right)/365\right) \\[2mm] t_h = t_{bj} + \left(LON - 120\right)/15 + E_Q/60 \\[2mm] E_Q = 0.0172 + 0.428cosQ_0 - 7.3515sinQ_0 - 3.3495cos(2Q_0) - 9.3619sin(2Q_0) \\[2mm] Q_0 = 2\pi(DOY - 1)/365 \end{cases} \qquad (3)$$

In the above calculation,

T_0 – Temperature at t_h ;

T_{max} – Highest daily temperature;

T_{min} – Lowest daily temperature;

dl – Length of a day (derived based on date and latitude)[20];

p – Time difference between the midday and the time of highest temperature (its value was assumed as 2 h in this study)[21];

LAT – Latitude;

DOY – Day of year constant;

δ – Solar declination;

t_h – Local solar time;

t_{bj} – Beijing standard time;

LON – Longitude;

E_Q – Corrected movement;

Q_0 – Solar declination angle.

The temperature data of ground weather stations was from the surface climate datasets of China available at the website of China Meteorological Data Sharing Service System (http://cdc.cma.gov.cn/home.do).

Studies have shown that the variation of atmospheric transmittance is solely associated with the dynamic change of atmospheric water vapor content. Therefore, the estimation of atmospheric transmittance is highly dependent on the atmospheric water vapor content [22]. Based on the characteristics of HJ-1B satellite, Duan *et al.* [7] proposed a revised estimation formula for atmospheric transmittance as below. In the equations, w is the atmospheric water vapor content.

$$\begin{cases} \tau = 0.9821 - 0.1241w \\ R^2 = 0.9667 \end{cases} \qquad (4)$$

1.1 RETRIEVAL OF ATMOSPHERIC WATER VAPOR CONTENT
Models like MODTRAN produce point-based results. An alternative approach was adopted in this study to obtain atmospheric water vapor content from MODIS data. A study of Meng *et al.* [20] showed that MODIS water vapor data is not necessarily applicable to small-scale areas, for which channel ratio method produces leads to higher accuracy in retrieving water vapor content. The MODIS image of the study area was generated at 11:00 of the same day, which is near the time that the HJ-1B satellite data was acquired. Therefore, the MOD021KM data was cut to fit the area of Guangzhou and retrieve the area's atmospheric water vapor content. Considering the bands of MOD021KM data, the method proposed by Sobrino [24] was adopted to retrieve the water vapor content. The equations are

$$\begin{cases} W_{17} = 26.314 - 54.434(L_{17} / L_2) + 28.449(L_{17} / L_2)^2 \\ W_{18} = 5.012 - 23.017(L_{18} / L_2) + 27.884(L_{18} / L_2)^2 \\ W_{19} = 9.446 - 26.887(L_{19} / L_2) + 19.914(L_{19} / L_2)^2 \\ w = 0.192W_{17} + 0.453W_{18} + 0.355W_{19} \end{cases} \quad (5)$$

In the above equations, L_2, L_{17}, L_{17} and L_{19} stand for the radiances of Band 2, 17, 18 and 19 of the MODIS imagery, respectively; W_{17}, W_{18} and W_{19} stand for the atmospheric water vapor contents of Band 17, 18 and 19, respectively; and w is the weighted mean of the estimated water vapor contents of the three bands.

1.2 RETRIEVAL OF EMISSIVITY

Many methods are available for the calculation of emissivity. With the emissivity information provided by the CCD embedded on HJ-1B, the emissivity of the fourth IRS band was determined using the widely recognized NDVI thresholding approach [25-27]. At the scale of 300 m, a reasonable partition of natural land surface is dividing it to pixels of vegetation, soil and their mix. When the image contains dense vegetation, the average NDVI value of the area could be used as the $NDVI_v$ value.

When $NDVI > NDVI_v$, the pixel was considered a vegetation pixel and its emissivity set to vegetation emissivity ε_v.

When $NDVI_s \leqslant NDVI \leqslant NDVI_v$, the pixel was considered a mixed pixel of vegetation and bare soil and the emissivity was calculated as $\varepsilon = \varepsilon_v P_v + \varepsilon_s(1 - P_v) + d\varepsilon$, where ε_v and ε_s are emissivity of vegetation and bare soil, respectively, P_v is the vegetation coverage, and $d\varepsilon$ describes the geometric structure of the mixed pixel and its internal scattering effect. The relation among the parameters is

$$\begin{cases} Pv = (NDVI - NDVI_s) / (NDVI_v - NDVI_s) \\ d\varepsilon = (1 - \varepsilon_s)\varepsilon_v F(1 - P_v) \end{cases} \quad (6)$$

When the land surface is level, the value of $d\varepsilon$ is roughly 0. The *F* in the equations is a terrain factor with a mean value of 0.55.

When $NDVI < NDVI_s$, the pixel was assumed as a bare soil pixel whose emissivity is determined by that of the infrared channel.

$\varepsilon = a\rho_R + b$, where ρ_R is the emissivity of CCD infrared channel, and *a* and *b* are regression coefficients. The emissivity of CCD infrared channel can be retrieved using the 6S atmospheric radiative transfer software.

With the 25 bare soil spectra included in the JohnsHopkinsUniversity JHU) spectrum base [28], and combining the spectrum response functions of the CCD1 and CCD2 channels of HJ-1B satellite, the emissivity and infrared emissivity of bare soil were calculated. A significant correlation at 0.02-level was revealed between the emissivity and infrared emissivity of bare soil; the correlation coefficients were 0.482 and 0.484, respectively. For CCD1 and CCD2, the values of *a* were -0.0274 and -0.0273, whereas the values of *b* were 0.9779 and 0.9779. The emissivity prediction error was in the range of -0.006 to 0.006. In the IRS channel, the emissivity of typical surface objects were 0.972, 0.983 and 0.988 for soil, vegetation and water, respectively.

2 ALGORITHM VALIDATION
2.1 STUDY AREA AND DATA SOURCE

Guangzhou is located in the south-central portion of Guangdong, China. North to the South China Sea and south to the Nanling Mountains, Guangzhou has a typical oceanic monsoon climate. Annual mean temperature ranges from 20 to 22 ℃, with an average relative humidity of 77%. Annual precipitation in the urban area of Guangzhou is around 1982.7 mm. The city spans from 112° 57' to 114° 35' E longitude and 22° 36' to 24° 04' N latitude.

Data selection was performed based on the variety of parameters needed by the algorithm. All the remote sensing images used were acquired on Jan 14, 2013. One grid of HJ-1B/CCD1 image (acquired at 10:45, orbit number 1/88), one grid of HJ-1B/IRS (acquired at 10:45, orbit number 3/86), one grid of MOD021KM remote sensing data and one grid of MOD11_L2 product data (11:00) were chosen for the study. The chosen images were in good quality

_____

with little cloud and clear surface features, and contained little interference.

2.2 LST RETRIEVAL RESULT AND VALIDATION

The MODIS temperature product MOD11_L2 with high precision (error < 1 K), provided by NASA, is often used as the standard to evaluate various algorithms' LST retrieval performance. The thermal infrared band resolution of HJ-1B data is 300 m, whereas the spatial resolution of MOD11_L2 product is 1 km. Therefore, the MOD11_L2 data was resampled to 300 m. Fig.1 displays the retrieved LST spatial distribution of Guangzhou and the MOD11_L2 data.
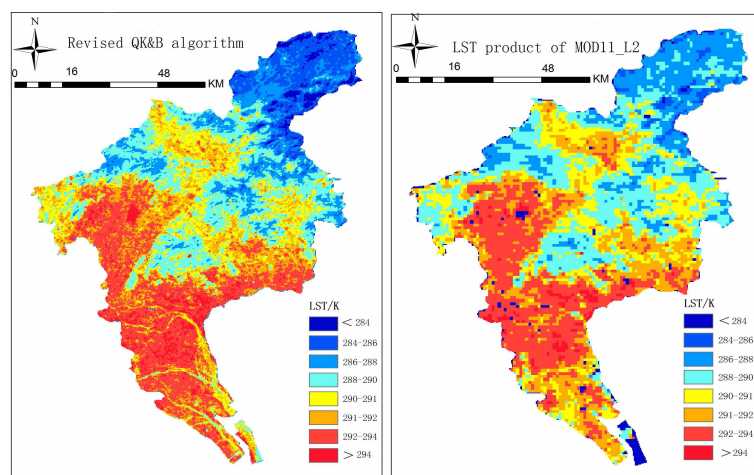
Fig.1 :Retrieved LST spatial distribution of Guangzhou and MOD11_L2 data

For the evaluation of LST retrieval algorithms, parametric errors [29] are often determined by simulating standard atmosphere with software packages that calculate atmospheric radiative transfer. One advantage of this approach is that full simulation of LST is not required. This approach only requires three sets of simulated LST, four sets of land surface emissivity, three sets of atmospheric temperature, three sets of atmospheric transmittance, and four or six types of standard atmosphere. The approach has been proved relatively accurate. However, the values of most parameters are presumed based on the atmospheric patterns prior to obtaining comprehensive error of different types of standard atmosphere and calculating mean error. Since the parameters in the algorithm are all plane pixel data with inconsistent values for different regions, it is not meaningful to validate the algorithms with just a few representative values. Therefore, the practical meaning and conviction of this approach are limited. In this study, the MOD11_L2 temperature product and the ground temperature measured from the filed were used to validate the accuracy of the retrieval algorithm. Difference between the LST of Guangzhou retrieved with the revised QK&B algorithm and the MOD11_L2 data provided by NASA is illustrated in Fig.2.
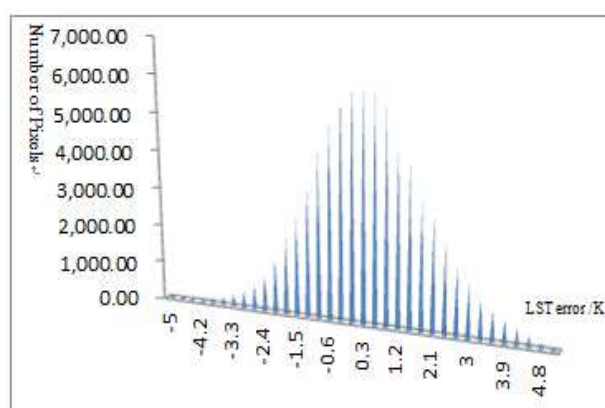
Fig.2 :Difference between LST retrieved by revised QK&B and MOD11_L2 data

As seen in Fig.2, the differences between the retrieved LST and the MODIS data follow a normal distribution, with most differences concentrated in the range of -0.9 to 0.9 K. A relatively high spatial consistency is shown between the retrieved LST of Guangzhou and the MOD11_L2 temperature data.

Considering that the low resolution of MODIS product may increase the difference of the algorithm and impact the accuracy, the surface data used must be able to represent the surface area covered by the remote sensing pixel in order to further validate the algorithm. Six observation areas of Guangzhou, including Tianhe park, campus of South China University of Technology, Baiyun Mountain, Guangzhou Tower, Guangzhou Olympic Stadium and Lianhua Mountain were chosen. Temperatures were taken at the six areas, respectively, between 10:40 to 11:10 in the morning of Jan 4th, 2013. The reason to choose this time period was that the HJ-1B/IRS passes by Guangzhou at 10:45 and the Terra satellite passes Guangzhou at 11:00. The land surface temperature temperature was recorded every 5 minutes in each area. After obtaining the temperature measurements, the mean temperatures were compared with the pixel temperature from MOD11_L2 data and the temperature retrieved with the algorithm. Taking the Tianhe park area as an example, the center of the area is located at 113°22'04'E and 23°07'36'N, it has a level terrain covered mostly by grassland, gardens, waters, and buildings. The measurers used portable GPS and portable thermal infrared radiometer to scan an area of 9 to 10 hm^2, consisting of 162 measuring spots, and recorded the surface temperature every 5 minutes at each spot. The average temperatures of all the measuring spots measured each round were then averaged. After a systematic analysis, the eventual LST comparison is as shown in Tab 1.

Tab. 1 Comparison of retrieved LST, MOD11_L2 data, and measured data

Observation area	Measured LST （K）	Geographic location	Retrieved LST	Products
			Revised QK&B (K)	MOD11_L2 (K)
Tianhe Park	292.93	113°22'04″ 23°07'36″	293.54	293.17
campus of SCUT	292.17	113°20'39″ 23°09'06″	292.76	292.57
Baiyun Mountain	290.51	113°17'42″ 23°10'59″	291.15	290.05
Guangzhou Tower	292.87	113°19'02″ 23°05'02″	293.91	293.45
Guangzhou Olympic Stadium	293.75	113°24'29″ 23°08'03″	293.06	294.94
Lianhua Mountain	293.11	113°30'01″ 22°58'30″	292.15	293.42
Mean	292.56		292.70	292.90

As seen in Tab.1, the LST retrieved with the revised QK&B algorithm, the MOD11_L2 data and the measured LST show good consistency. An average difference of 0.31 K is shown between the retrieved LST and the measured LST, and an average difference of 0.65 K is shown between the retrieved LST and the MODIS-LST data. Generally, the measured LST is very close to the MODIS data for most observation areas, except for Guangzhou Olympics Stadium, where a difference of 1.19 K exists. This may be attributed to that the area is close to the urban area of Guangzhou, where the emission of traffic exhaust gas is high and the vegetation is sparse. For Lianhua Mountain, which is the least influenced by vegetation and water, the difference between the measured LST and the MODIS data is only 0.31 K. Meanwhile, the retrieved LST and the measured LST exhibit the difference as high as 1.14 K for the Guangzhou Tower area. The temperatures of other observation areas were relatively close to the retrieved LST with errors less than 1 K. A good result of applying the revised QK&B algorithm to the monitoring and analysis of Guangzhou's heat island effect was demonstrated.

3 PARAMETER SENSITIVITY IN LST RETRIEVAL FROM HJ-1B/IRS DATA

Generally, the sensitivity of LST retrieval to parameter errors can be calculated with the following equation [15, 31].

$$\Delta T_s = \left| T_s\left(x + \Delta x\right) - T_s\left(x\right) \right| \qquad (7)$$

where $T_s\left(x + \Delta x\right)$ and $T_s\left(x\right)$ are the retrieved land surface temperatures corresponding to parameters $(x + \Delta x)$ and (x), respectively, ΔT_s is the LST retrieval error, and Δx is the estimation error of parameter x. Considering the capability of partial differential equation of reflecting change rate, partial differential equations were established for all parameters to perform sensitivity analysis, where the influence of each parameter's error on the retrieval of T_s was analyzed.

3.1 THE FACTOR OF EMISSIVITY

The LST retrieval error $e_\varepsilon\left(T_s\right)$ caused by emissivity estimation error $e(\varepsilon)$ was derived through the partial differential equation based on the revised QK&B algorithm.

$$e_\varepsilon(T_s) = \left[\frac{\delta T_s}{\delta \varepsilon}\right] e(\varepsilon)$$

$$= \left[(-1)\frac{a\tau}{\varepsilon^2} + (1-b)T_{sensor}\frac{\tau}{\varepsilon^2} - \frac{T_{sensor}}{\varepsilon^2\tau} + \frac{T_a}{\varepsilon^2\tau} - \frac{T_a\tau}{\varepsilon^2}\right] e(\varepsilon) \qquad (8)$$

Based on the above equation, the LST error caused by the emissivity error was investigated. The equation was imported into ENVI-IDL program and the relation between LST error and the emissivity error as shown in Fig.3 was obtained. During the process, the values of all other parameters of the QK&B algorithm were kept the same with the parameter setup (plane pixel values) so that the error in the obtained LST is resulted from emissivity error only.
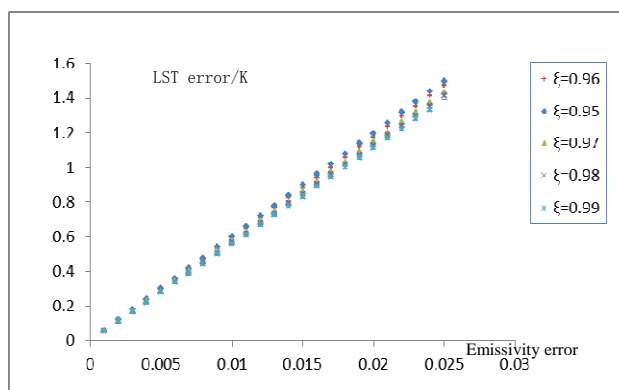
Fig.3 :Probable LST estimation error because of the possible emissivity error

As seen in Fig.3, the LST error decreases with the emissivity and increases with the error in emissivity. The diagram shows five different values of the emissivity. When the error in the emissivity was 0.01, the resultant LST errors at all five values of emissivity was 0.6 K. In addition, when the s emissivity changed from 0 to 0.03, the resultant LST error was always in the range of 0 to 1.5 K. Therefore, we can conclude that the variation of emissivity has little influence on LST retrieval error.

3.2 THE FACTOR OF ATMOSPHERIC TRANSMITTANCE

Similarly, the LST error $e_\tau(T_s)$ caused by atmospheric transmittance error $e(\tau)$ was derived based on the revised QK&B algorithm:

$$e_\tau(T_s) = \left[\frac{\delta T_s}{\delta \tau}\right] e(\tau)$$

$$= \left[\frac{a}{\varepsilon}(1-\varepsilon) + \frac{T_{sensor}}{\varepsilon}(1-\varepsilon)(b-1) - \frac{T_{sensor}}{\varepsilon\tau^2} + \frac{T_a}{\varepsilon\tau^2} + \frac{T_a}{\varepsilon} - T_a\right] e(\tau) \qquad . \quad (9)$$

The relationship between atmospheric transmittance error and LST retrieval error was investigated and plotted as Fig.4, with other parameters kept constant.
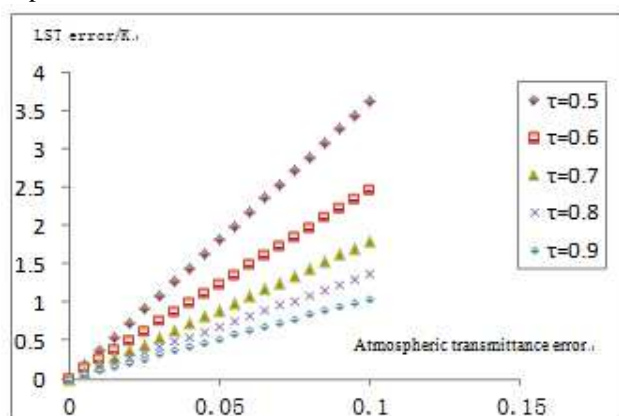
Fig.4:Probable LST estimation error because of the possible atmospheric transmittance error

As seen in Fig.4, the variation of atmospheric transmittance has a relatively high influence on LST error. Generally, LST error is inversely proportional to atmospheric transmittance and proportional to atmospheric transmittance error. At the transmittance of 0.5, the LST error caused by transmittance error of 0 to 0.1 was around 3.6 K. When the transmittance is 0.9, the LST error caused by transmittance error of 0 to 0.1 was around 1 K. We can conclude that the variation of atmospheric transmittance has significant influence on LST retrieval error. Therefore, the error in transmittance should be kept under 0.1 through precise and strict computation.

3.3 THE FACTOR OF AVERAGE ATMOSPHERIC TEMPERATURE

The LST error $e_{T_a}(T_s)$ caused by the error in average atmospheric operative temperature $e(T_a)$ is

$$e_{T_a}(T_s) = \left[\frac{\delta T_s}{\delta T_a}\right]e(T_a) = \left[(-1)\frac{(1-\tau)\left[1+(1-\varepsilon)\tau\right]}{\varepsilon\tau}\right]e(T_a). \quad (10)$$

As Equation (10) shows, at a constant value of $\left[(-1)\dfrac{(1-\tau)\left[1+(1-\varepsilon)\tau\right]}{\varepsilon\tau}\right]$, LST error is irrelevant to the value of average atmospheric operative temperature but associated with its error. Therefore, a ratio relation between atmospheric transmittance and emissivity was studied in order to obtain the LST error resulting from the variation of average atmospheric operative temperature. Since τ and ε are two unknown variables whose relationship needs to be determined to understand the LST error, the two influencing factors discussed above, atmospheric transmittance and emissivity, were utilized. The ratio relation between them was obtained and the resultant LST error is as shown in Fig.5 and Tab.2

Tab.2 Relationship ratio of land surface emissivity and atmospheric transmittance factor

Surface emissivity ε	Atmospheric transmittance τ	$C = \varepsilon\tau$	$D = (1-\tau)\left[1+(1-\varepsilon)\tau\right]$	$\dfrac{D}{C}$
0.95	0.5	0.475	0.5125	1.078947
0.96	0.5	0.48	0.51	1.0625
0.97	0.5	0.485	0.5075	1.046392
0.98	0.5	0.49	0.505	1.030612
0.99	0.5	0.495	0.5025	1.015152
0.95	0.6	0.57	0.412	0.722807
0.96	0.6	0.576	0.4096	0.711111
0.97	0.6	0.582	0.4072	0.699656
0.98	0.6	0.588	0.4048	0.688435
0.99	0.6	0.594	0.4024	0.677441
0.95	0.7	0.665	0.3105	0.466917
0.96	0.7	0.672	0.3084	0.458929
0.97	0.7	0.679	0.3063	0.451105
0.98	0.7	0.686	0.3042	0.44344
0.99	0.7	0.693	0.3021	0.435931
0.95	0.8	0.76	0.208	0.273684
0.96	0.8	0.768	0.2064	0.26875
0.97	0.8	0.776	0.2048	0.263918
0.98	0.8	0.784	0.2032	0.259184
0.99	0.8	0.792	0.2016	0.254545
0.95	0.9	0.855	0.1045	0.122222
0.96	0.9	0.864	0.1036	0.119907
0.97	0.9	0.873	0.1027	0.11764
0.98	0.9	0.882	0.1018	0.11542
0.99	0.9	0.891	0.1009	0.113244

As seen in Fig.5 and Tab.2, LST error varies with the error in average atmospheric operative temperature; the maximum LST error is 6 K, which is not permissible in LST retrieval. When the ratio relation between the emissivity and atmospheric transmittance is constant, LST error is proportional to the error in average atmospheric operative error. Generally, LST error is proportional to the ratio. The ratio can be divided into five intervals, 0.113~0.122, 0.255~0.277, 0.435~0.466, 0.67~0.72 and 1.01~1.07. When the ratio varied in the first interval, as the average atmospheric operative temperature error changed from 0.5 K to 4.5 K, the resultant LST error only changed for less than 1 K. When the ratio was in the intervals of 0.67~0.73 and 1.01 to 1.07, the variation of average atmospheric operative temperature error from 0.5 K to 4.5 K resulted in LST error of 0.25 to 3.8 K and 0.5 to 5.6 K, respectively. Therefore, in addition to control the average atmospheric operative temperature within a reasonable range during LST retrieval, this ratio relation between surface emissivity and atmospheric transmittance should also be considered. By considering both factors, the LST error caused by error in average atmospheric operative temperature can be reduced significantly.
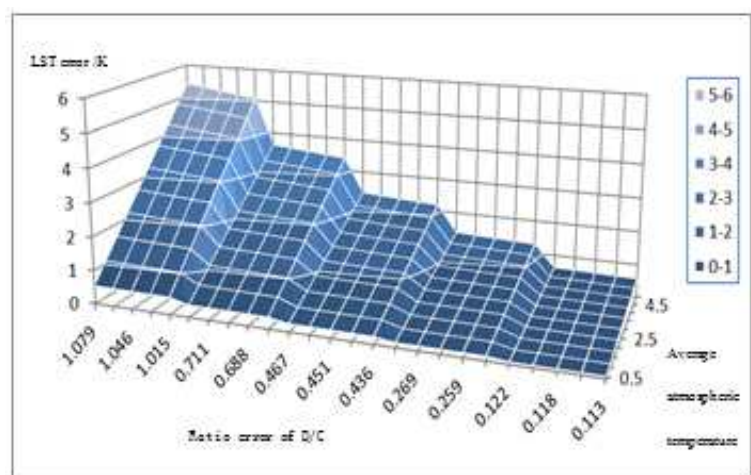
Fig.5:Probable LST estimation error because of the possible average atmospheric temperature error

3.4 THE FACTOR OF ATMOSPHERIC WATER VAPOR CONTENT

The LST error $e_w(T_s)$ caused by error in the estimation of atmospheric water vapor content

$$
e_w(T_s) = \left[\frac{\delta T_s}{\delta w}\right] e(w)
$$

$$
= \left[\begin{array}{l} \dfrac{a}{\varepsilon}(1-\varepsilon)(-0.1241) + \dfrac{T_{sensor}}{\varepsilon}(1-\varepsilon)(b-1)(-0.1241) + \dfrac{T_{sensor}}{\varepsilon\tau^2}(0.1241) \\[2mm] + \dfrac{T_a}{\varepsilon\tau^2}(-0.1241) + \dfrac{T_a}{\varepsilon}(-0.1241) + 0.1241 Ta \end{array}\right] e(w) \qquad (11)
$$
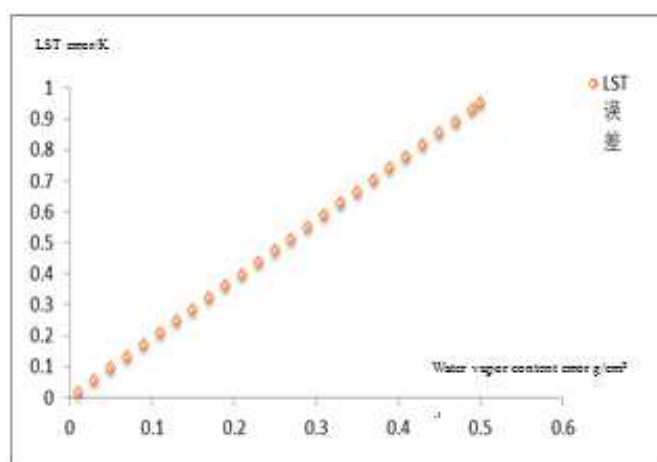
Fig.6:Probable LST estimation error because of the possible water vapor content error

After the partial differential derivation, the LST error caused by the error in atmospheric water vapor content *w* was calculated as shown in Fig. 6. A linear relationship can be seen. When the atmospheric water vapor error is 0.1 g/cm^2, the resultant LST error was about 0.2 K, and the increase of the former to 0.5 g/cm^2 resulted in an LST error of 0.2 to 1 K. As the LST error resultant from 0.5 g/cm^2 of water vapor error was 1 K, the influence of water vapor error on LST retrieval error was considered high. Therefore, the water vapor error should be kept under 1 g/cm^2 during LST retrieval in order to reduce this influence.

3.5 THE FACTOR OF NEAR-SURFACE TEMPERATURE

The LST error $e_{T_0}(T_s)$ caused by near-surface temperature estimation error $e(T_0)$ (calculated with partial differential equation of the revised QK&B algorithm) is

$$e_{T0}(T_s) = \left[\frac{\delta T_s}{\delta T_0}\right] e(T_0)$$

$$= -0.88894 \left[\frac{1 - \varepsilon\tau - \tau^2 + \varepsilon\tau^2}{\varepsilon\tau}\right] e(T_0) \tag{12}$$

As Equation (12) shows, when the error in near-surface temperature is maintained at $-0.88894\left[\frac{1-\varepsilon\tau-\tau^2+\varepsilon\tau^2}{\varepsilon\tau}\right]$, the resultant LST error is only related to the error, despising the value of the temperature. On the basis of the relationship between atmospheric transmittance and emissivity, the relationship between LST error and near-surface air temperature error was plotted as in Fig.7.
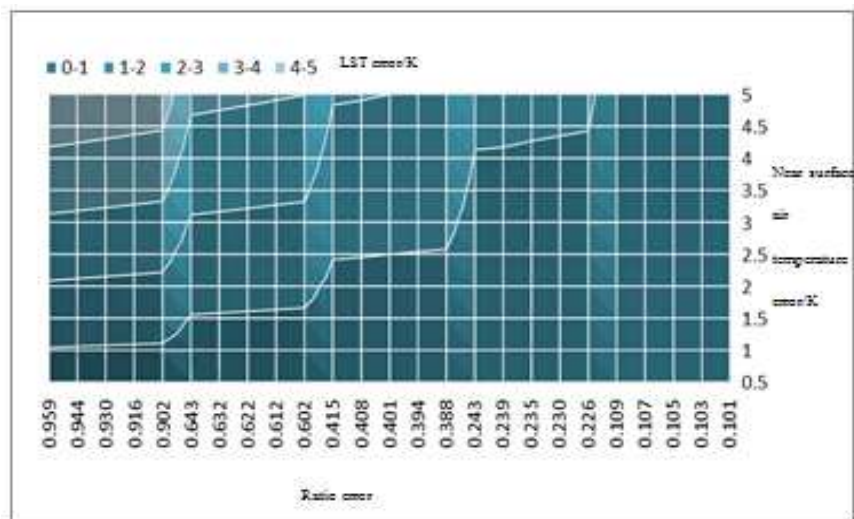
Fig. 7 Probable LST estimation error because of the possible near surface air temperature error

As seen in Fig.7, when the error in near-surface air temperature varied in the range of 0.5~5 K, the resultant LST error was in the range of 0~5 K. Generally, at a constant ratio relation between emissivity and atmospheric transmittance, LST error increases with near-surface air temperature error. When the ratio was in the range of 0.101 to 0.109, the LST error changed only slightly with the near-surface temperature error in the range of 0 ~ 1 K. When the ratio was in other ranges, the LST error exhibited different degrees of fluctuation with near-surface air temperature error. When the ratio was in the range of 0.902 to 0.959, LST error varied significantly in the range of 0~5 K as the near-surface air temperature error changed from 0.5 K to 5 K, and the near-surface air temperature error of 1 K resulted in LST error of about 1 K. Therefore, both the ratio relation between emissivity and atmospheric transmittance and the near-surface air temperature error should be controlled in lower ranges in order to reduce LST error.

CONCLUSION

In this study, a revised QK&B algorithm was adopted to perform error analysis of the land surface temperature (LST) retrieval with data from HJ-1B/IRS remote sensing data. The algorithm was chosen based on responsive characteristics of the thermal infrared band of HJ-1B satellite. With the remote sensing data, the LST distribution of Guangzhou on Jan 14, 2013 was retrieved. The plane pixel of a temperature product and the field measured surface temperature were used to validate the algorithm. The temperature product was MODIS, which was used to interpolate the retrieved LST. The difference between the retrieved LST and the MODIS-LST data was in the range of -0.9K~0.9K with a normal distribution. The difference between the retrieved LST and the measured LST was 0.32 K, and the difference between the measured LST and the MODIS-LST data was 0.65 K. A high precision of the revised QK&B algorithm was demonstrated.

Based on the principle of rate of change, partial differential equation was established for sensitivity analysis. Error analysis was performed for LST retrieval in terms of five influencing factors. The partial differential equation derived from the algorithm showed that emissivity has insignificant influence on LST retrieval error; The emissivity error of 0.01 led to LST error of about 0.6 K, whereas the variation of emissivity error from 0 to 0.03 led to LST error in the range of 0 ~ 0.5 K. Meanwhile, LST error is inversely proportional to atmospheric transmittance and

proportional to the error in atmospheric transmittance; the transmittance error of 0.1 resulted in LST error of 1 K, which is relatively large. When the ratio relation between emissivity and atmospheric transmittance is constant, LST retrieval error is only associated with the error in average atmospheric operative temperature. The ratio of emissivity to atmospheric transmittance is in a ladder distribution; when the ratio was in the ranges of 0.67~0.73 and 1.01~1.07, the variation of average atmospheric operative temperature from 0.5 to 4.5 K resulted in LST error of 0.25 to 3.8 K and 0.5 to 5.6 K, respectively. As of the atmospheric water vapor content, a linear relationship was found between its error and the resultant LST error; when the error of water vapor content was 0.1 g/cm^2, the resultant LST error was about 0.2 K. Near-surface temperature was another influencing factor; the variation of near-surface temperature error from 0.5 to 5 K led to LST error in the range of 0 to 5 K. At constant ratio relation between emissivity and transmittance, the LST retrieval error generally increased with the increase of near-surface temperature error. When the ratio was in the range of 0.902~0.959, the variation of near-surface temperature error from 0.5 to 5 K led to LST error of 0 to 5 K, where 1 K of surface temperature error could result in LST error of near 1 K.

Through the error analysis presented in this paper, the generation and transfer patterns of error in LST retrieval with the revised QK&B algorithm from HJ-1B thermal infrared data was revealed. This paper provides a reference for the error analysis of similar LST retrieval algorithms that retrieve LST from environment thermal infrared band satellites or other satellite sensors. In addition, a scientific basis is offered for further error reduction and accuracy improvement of LST retrieval.

REFERENCES

[1]Dash P, Göttsche F M, Olesen F S, et al. *theory and practice-current trends*.**2002**,12(15),2563-2594.
[2]Jiménez-Muñoz J C, Sobrino J A. *Journal of Geophysical Research Atmospheres*.**2003**,17(12),4673- 4688.
[3] Wan Z, Li Z *IEEE Transactions on Geoscience & Remote Sensing*. **1997**,35(4) ,980-992.
[4] Zhuang Jiali, Xu Xiru, Chen Liangfu, et al. *method based on evolution Science in China(Series D)*. **2001** ,24(01),81-88.
[5] Liu Sanchao, Gao Maofang, Qin Zhihao. *Remote Sensing Information*. **2005**,18(06),3-12.
[6] Xu Hanqiu, Ding Feng, et al. *Science of Surveying and Mapping*. **2007**,12(01),87-90.
[7] Li Xiaowen, Duan Sibo, Yan Guangjian, et al *Progress in Natural Science*. **2008**,27(09),1001-1008.
[8] Guo Jianxia, Zhou Ji, Li Jing, et al *Journal of Infrared and MillimeterWaves*.**2011**,15(01),61-67.
[9] Sobrino J A, Jiménez-Muñoz J C, Paolini L *Remote Sensing of Environment*. **2004** ,90(4), 434-441.
[10] Sobrino J A, Jiménez Muñoz J C. *Journal of Geophysical Research* .**2005**,110(D16),1102-1113.
[11] Sobrino J A, Jiménez-Muñoz J C, El-Kharraz J, et al. *International Journal of   Remote Sensing*. **2004** ,25(1),215-230.
[12]Wang Changzuo, Huang Miaofen, Xing Xufeng. *Arid Land Geography* .**2006**, 15(01), 132-137.
[13] Yang J, Gong P, Zhou J, et al. *Science of Surveying and Mapping*.**2010**,53(1),67-73.
[14] Liu Rui, Yang Peiguo, Hu Junfeng. *Science of Surveying and Mapping*. **2013** ,16(01), 60-62.
[15] Zhou J, Zhan W, Hu D, et al. Improvement of mono-window algorithm for retrieving land surface temperature from HJ-1B satellite data. **2010**,20(2),123-131.
[16] Meng Dan, Li Yanfang, Li Xiaojuan. *Journal of Capital Normal University*,**2010**,15(03):70-75.
[17] Wang Zhishun, Gao Wenlan, Li Xintong. *Science China: Information Sciences*. **2011**,27(112),89-98.
[18] Qin Z, Karnieli A, Berliner P. *International Journal of Remote Sensing*. **2001** ,22(18): 3719-3746.
[19] Berliner, Qin Zhihao, Li Wenjuan *Remote Sensing for Land & Resources*. **2003**,51 (02),37-43.
[20] Zhang Tangtang，Meng Xianhong Lv Shihua. *Plateau Meteorology*. **2005** ,42(05),721-726
[21] Sobrino J A, Kharraz J E *International Journal of Remote Sensing*. **2003**,24(24), 5161-5182
[22] Sobrino J A, Raissouni N, Li Z. *Remote Sensing of Environment*. **2001** ,75(2), 256-266.
[23] Coll C, Caselles V, Valor E, et al *Remote Sensing of Environment*. **2012**,117(13), 199-210.
[24] Liu Jia, Qin Zhihao, Li Wenjuan. *Remote Sensing for Land & Resources* . **2004** ,15(03),28-32.
[25] Berk A, Anderson G P, Acharya P K, et al *Space Vehicles Directorate*., **1999**,86(14),1-5.
[26] Yu Qin, Mao Kebiao, Qin Zhihao. *Journal of China University of Mining & Technology*. **2005** ,74(03): 318-322.
[27] Qin Z, Karnieli A, Berliner P *International Journal of Remote Sensing*. **2001** ,22(18): 3719-3746.
[28] Qin Z, Dall'Olmo G, Karnieli A, et al. *Journal of Geophysical Research: Atmospheres*., **2001**,106(D19): 2655-2670.